PHYSICAL REVIEW B VOLUME 45, NUMBER 23 15 JUNE 1992-I

Quantitative study of atomic ordering in $Ga_{0.5}In_{0.5}P$ thin films by ^{31}P nuclear magnetic resonance

Robert Tycko and Gary Dabbagh
AT&T Bell Laboratories, 600 Mountain Avenue, Murray Hill, New Jersey 07974

Sarah R. Kurtz and John P. Goral
National Renewable Energy Laboratory, 1617 Cole Boulevard, Golden, Colorado 80401

(Received 6 December 1991)

We use ^{31}P nuclear-magnetic-resonance (NMR) spectra to measure the degree of cation ordering in thin films of the semiconductor alloy $Ga_{0.5}In_{0.5}P$ grown by organometallic vapor-phase epitaxy. We show that the five possible $Ga_nIn_{4-n}P$ clusters in $Ga_xIn_{1-x}P$ give rise to resolved NMR lines under magic-angle spinning, allowing a determination of the degree of cation ordering from the relative areas of the five lines. The ordering is shown to be weak (order parameter ≤ 0.6) even in films that appear highly ordered in transmission electron microscopy.

I. INTRODUCTION

Atomic ordering in III-V semiconductor alloys is a widely studied phenomenon.[1-7] In $Ga_xIn_{1-x}P$, evidence from transmission electron microscopy (TEM) (Refs. 2-6) and other sources[8-11] indicates that the cations (Ga and In) are not distributed randomly on the group-III sublattice in thin films grown by organometallic vapor-phase epitaxy (OMVPE); instead, there exist domains in which the cations order on $(\bar{1}11)$ or $(1\bar{1}1)$ planes.[2-6] Figure 1 shows random and fully ordered structures. Atomic ordering is thought to result from surface thermodynamic and kinetic effects involved in the film-growth process.[10,12-15] It has been proposed that variations in the degree of atomic ordering are responsible for observed variations in the band gap,[3,16] and that the degree of atomic ordering can be controlled by varying the growth conditions.[3,10,14] Although there is considerable evidence that ordering is related to the optical properties, with more highly ordered material having a lower band gap, the band-gap depression predicted for a perfectly ordered alloy compared with a random alloy [0.26 eV (Ref. 17)] exceeds the largest band-gap variations observed [0.1 eV (Refs. 14 and 18)]. A clearer understanding of the origin of atomic ordering in $Ga_{0.5}In_{0.5}P$ and of the influence of atomic ordering on the electronic and optical properties has been hindered by the lack of quantitative experimental measurements of the degree of ordering in real films. Only one quantitative TEM study has appeared, in which the order parameter S (defined below) is reported to be 0.4 or less in $Ga_{0.5}In_{0.5}P$ films with unspecified band gaps and growth conditions.[6] On the other hand, it has sometimes been assumed that the ordering is complete ($S \approx 1$) within the ordered domains that appear in TEM.[2] In this paper, we demonstrate that ^{31}P nuclear-magnetic-resonance (NMR) spectra, obtained with magic-angle spinning (MAS), [19] can be used to measure the degree of cation ordering in $Ga_xIn_{1-x}P$ thin films. Our NMR spectra of $Ga_{0.5}In_{0.5}P$ films indicate that the *atomic ordering is not strong* ($S \leq 0.6$) *even in films that appear highly ordered in TEM.*

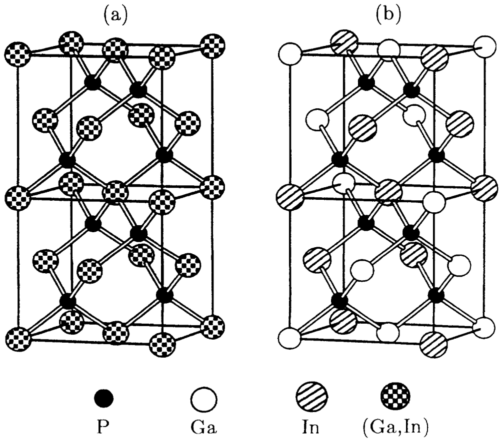

FIG. 1. (a) Random and (b) fully ordered $Ga_{0.5}In_{0.5}P$ structures.

II. EXPERIMENTAL METHODS

$Ga_{0.5}In_{0.5}P$ films were grown by atmospheric pressure OMVPE using trimethylgallium, trimethylindium, and phosphine in a hydrogen carrier gas.[14] Films were 7-15 μm thick and 2×2 cm^2. The composition was measured by double-crystal x-ray diffraction to be within 1% of the lattice-matched composition ($Ga_{0.515}In_{0.485}P$). Carrier concentrations were $(1-5)\times10^{16}$ cm^{-3}. Band gaps were measured from the spectral dependence of the photocurrent generated at an electrolyte-semiconductor junction. Four films were prepared, with growth conditions that sample different regions of parameter space.[14] Growth rates were 6 μm/h for samples A, B, and D, and 3 μm/h for sample C. Inlet group-V- to group-III-atom ratios were 70 for A, B, and D, and 25 for C. Growth temperatures were 600, 670, 625, and 690 °C for A, B, C, and D, respectively. Samples B, C, and D have low band gaps (1.81-1.82 eV). Sample A has a relatively high band gap (1.88 eV). TEM measurements were carried out on sample *D* as described below.

$Ga_{0.5}In_{0.5}P$ films were ground to powders for ^{31}P NMR measurements after etching away the GaAs substrate with aqueous NH_3 and H_2O_2. The mild procedure used to grind the films is expected to have no effect on atomic ordering. Sample weights ranged from 5 to 12 mg. Spectra were obtained at room temperature on a Chemagnetics CMX spectrometer operating at 161.7 MHz (9.39-T field), using a home-built probe with a Doty Scientific sample spinning assembly. ^{31}P spin-lattice relaxation times (T_1) were measured with the saturation-recovery technique and were roughly 100 s. T_1 was constant across the spectrum. Transverse relaxation times (T_2) were measured from spin-echo decays using a $90°$-τ-$180°$-τ sequence, with τ incremented in units of the sample spinning period. T_2 was not constant across the spectrum, as described below.

III. RESULTS AND DISCUSSION

The potential sensitivity of ^{31}P NMR spectra to cation ordering arises from the dependence of the ^{31}P chemical shift (resonant frequency) on the identities of nearest neighbors. Since a ^{31}P atom in $Ga_xIn_{1-x}P$ can have n Ga and 4-n In nearest neighbors, we expect the ^{31}P NMR spectrum of $Ga_xIn_{1-x}P$ to show five lines in general. The relative areas A_n of the lines would then be proportional to the populations of $Ga_nIn_{4-n}P$ clusters in the sample, which in turn would depend on the degree of ordering.[20] A partially ordered structure in which alternating $\{111\}$-type planes in the group-III sublattice have compositions $Ga_{x+y}In_{1-x-y}$ and $Ga_{x-y}In_{1-x+y}$ is consistent with the TEM and other results. The order parameter is then defined by $S=2y$. Figure 1(b) shows the extreme case of $S=1$ for $x=0.5$, while Fig. 1(a) represents $S=0$. For a partially ordered alloy, the relative areas of the ^{31}P NMR lines would be

$$\begin{aligned}
A_0 &= 0.5[(x-y)(x+y)^3+(x+y)(x-y)^3]\,,\\
A_1 &= 0.5[(1-x+y)(x+y)^3+(1-x-y)(x-y)^3]\\
&\quad +1.5[(1-x-y)(x-y)(x+y)^2\\
&\qquad +(1-x+y)(x+y)(x-y)^2]\,,\\
A_2 &= 1.5[(x-y)(x+y)(1-x-y)^2\\
&\quad +(x+y)(x-y)(1-x+y)^2\\
&\quad +(x+y)(x-y)(1-x+y)^2\\
&\quad +(1-x+y)(1-x-y)(x+y)^2]\,, \qquad (1)\\
A_3 &= 0.5[(x-y)(1-x-y)^3+(x+y)(1-x+y)^3]\\
&\quad +1.5[(x+y)(1-x+y)(1-x-y)^2\\
&\qquad +(x-y)(1-x-y)(1-x+y)^2]\,,\\
A_4 &= 0.5[(1-x+y)(1-x-y)^3\\
&\quad +(1-x-y)(1-x+y)^3]\,.
\end{aligned}$$

In earlier ^{31}P NMR studies of InP, GaP, and $Ga_xIn_{1-x}P$, only a single line was observed,[21-23] indicating that the ^{31}P lines from the five types of $Ga_nIn_{4-n}P$ clusters are too broad to be resolved from one another and that information about cation ordering is therefore inaccessible. However, we realized that the contributions to the linewidths from homonuclear and heteronuclear magnetic dipole-dipole couplings and from the anisotropy of the ^{31}P chemical shift should be averaged out in high-field NMR by rapid MAS,[19] which was not employed in the earlier studies. The effect of MAS on the ^{31}P NMR spectrum of a bulk, polycrystalline sample of $Ga_{0.14}In_{0.86}P$ is shown in Fig. 2. Assuming a random distribution of cations, as expected for a bulk sample, the (integrated) areas under the lines are expected to be in the ratios 0.000:0.009:0.087:0.356:0.547 (in order of decreasing n). Under rapid MAS, three main lines of significant intensity are, in fact, resolved. As is typical of MAS spectra, there are also auxiliary lines (spinning sidebands) separated from the main lines (center bands) by multiples of the spinning frequency ν_{MAS}. A least-squares fit to the

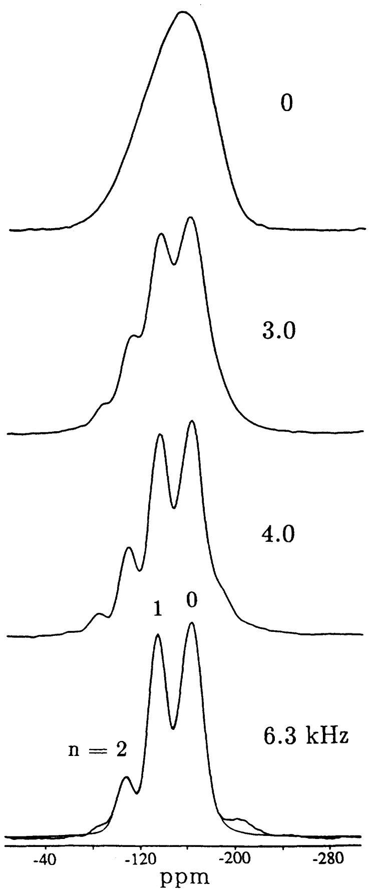

FIG. 2. ^{31}P MAS NMR spectra of bulk, polycrystalline $Ga_{0.14}In_{0.86}P$ at the indicated sample spinning frequencies. A least-squares fit, as described in the text, is superimposed on the spectrum at $\nu_{MAS}=6.3$ kHz. The assignment of NMR lines to $Ga_nIn_{4-n}P$ clusters, also described in the text, is indicated. Frequencies are in ppm with respect to 85% H_3PO_4, with higher frequencies to the left.

spectrum at $\nu_{\rm MAS}=6.3$ kHz, assuming three lines, yields relative areas 0.09:0.38:0.53, in good agreement with the ratios predicted for the three most intense lines in a random structure with $x=0.14$. In the fitting procedure, the width, center frequency, and area of each line are allowed to vary. A convoluted Gaussian-Lorentzian line shape is used, with a ratio of Lorentzian to Gaussian broadening that is variable but the same for all lines in the spectrum. Although the experimental spectrum at $\nu_{\rm MAS}=6.3$ kHz shows five lines, we fit only the three most intense lines because the line at -205 ppm is entirely a spinning sideband the the line at -85 ppm, which we assign to $n=3$, is not well resolved and may contain contributions from spinning sidebands (see the discussion of assignments below).

Our results on *bulk* $\mathrm{Ga}_x\mathrm{In}_{1-x}\mathrm{P}$ encouraged us to attempt NMR measurements on $\mathrm{Ga}_x\mathrm{In}_{1-x}\mathrm{P}$ *thin films.* Figure 3 shows the ^{31}P NMR spectra of the four $\mathrm{Ga}_{0.5}\mathrm{In}_{0.5}\mathrm{P}$ films. Five lines (five centerbands) are observed, although the outer lines are not always well resolved. Least-squares fits to the experimental spectra are superimposed. In these fits, the spectra are assumed to consist of five lines with variable center frequencies and linewidths, as above. The areas of the five lines are constrained to be in the ratios 0.070:0.265:0.374:0.235:0.055, appropriate for a random alloy with $x=0.515$. The fact that good fits can be obtained indicates that *the cation ordering is not strong in any of the samples.* More precisely, the NMR spectra place an upper bound on S. To determine this bound, we calculated a series of least-squares fits to the experimental spectra with the areas of the five lines constrained to satisfy Eq. (1) for values of S between 0 and 1. Figure 4(a) shows the dependence of $\{A_n\}$ on S given by Eq. (1). Figure 4(b) shows the mean-squared deviation of the least-squares fit as a function of S for each of the four films, normalized to the mean-squared deviation for $S=0$. The fits become markedly worse for $S>0.6$, indicating that $S\leq 0.6$ in all four films. Figure 5 shows the calculated least-squares fits to the experimental spectrum of sample C for several values of S, illustrating the sensitivity of the fitting procedure to the assumed value of S. As S increases, the fitting procedure adjusts the linewidths in such a way that the peak heights appear not to change dramatically, even though the peak areas are changing as shown in Fig. 4(a).

Good fits to the experimental ^{31}P NMR spectra cannot

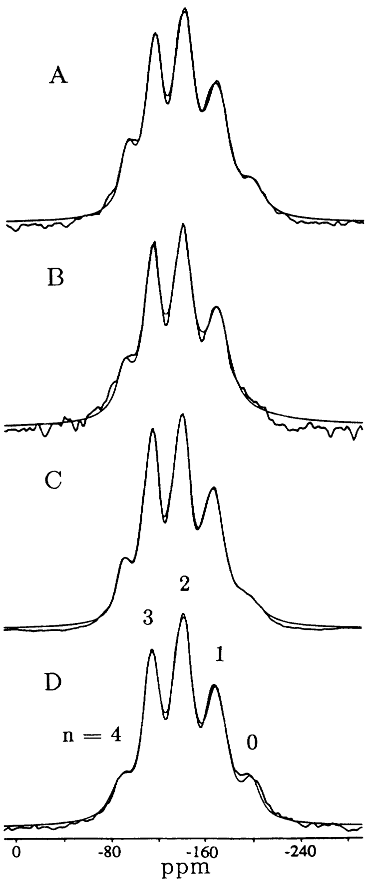

FIG. 3. ^{31}P MAS NMR spectra of $\mathrm{Ga}_{0.5}\mathrm{In}_{0.5}\mathrm{P}$ films grown under conditions described in the text. Least-squares fits that assume a random distribution of cations are superimposed. $\nu_{\rm MAS}=6.0$, 6.0, 6.5, and 5.0 kHz for samples A–D, respectively. (Assignments indicated as in Fig. 2.)

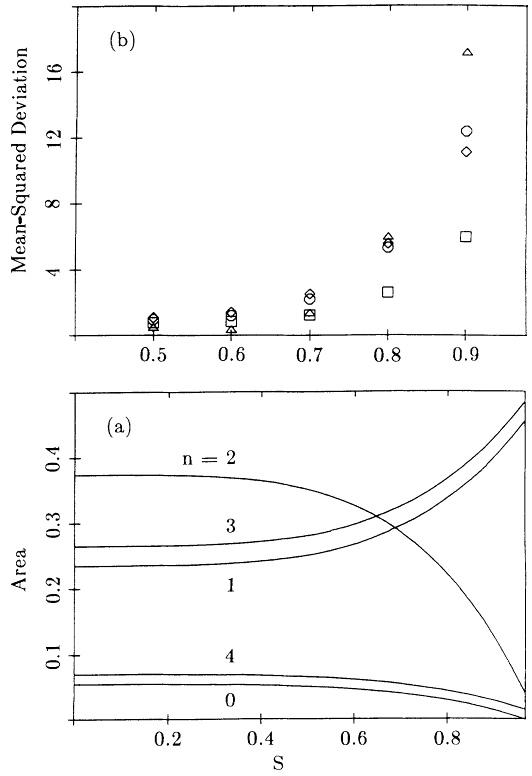

FIG. 4. (a) Calculated dependence on the order parameter S of the relative areas of the lines from the five possible $\mathrm{Ga}_n\mathrm{In}_{4-n}\mathrm{P}$ clusters in the ^{31}P NMR spectrum of $\mathrm{Ga}_{0.515}\mathrm{In}_{0.485}\mathrm{P}$. (b) Mean-squared deviation of the least-squares fits to the four spectra in Fig. 3 as a function of the assumed order parameter. The fits become markedly worse when S is assumed to be greater than 0.6. (A, octagon; B, square; C, triangle; D, diamond.)

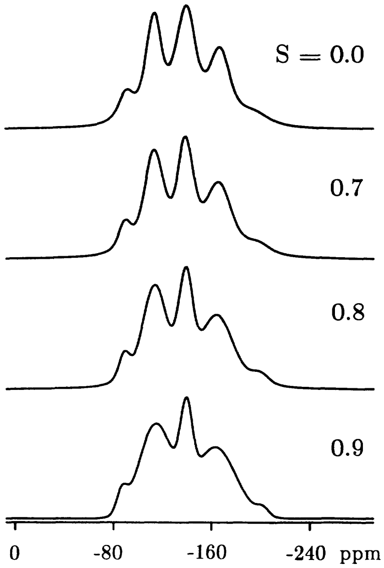

FIG. 5. Least-squares fits to the experimental ^{31}P NMR spectrum C in Fig. 3 in which the indicated values of the order parameter S are assumed. The spectrum calculated for $S=0.5$ is the same as the one superimposed on the experimental spectrum C in Fig. 3.

be obtained without allowing the linewidths of individual resonance lines to vary independently. That this is true is evident from the fact that the lines from the $Ga_nIn_{4-n}P$ clusters with $n=1$ and 3 in Fig. 3 have significantly different peak heights, although their areas are nearly equal. The residual linewidths in our MAS spectra are due to the sensitivity of the ^{31}P chemical shift to the identities and arrangement of next-nearest-neighbor and more distant cations. It is apparent that the chemical shift of a P nucleus in a $GaIn_3P$ cluster is affected more strongly by the next-nearest-neighbor and more distant cations than the chemical shift of a P nucleus in a Ga_3InP cluster, since the $n=1$ line is broader. We can offer no explanation for this observation.

For large S (e.g., $S=0.9$), the normalized mean-squared deviations in Fig. 4(b) are different for the four films. This difference does not in itself reflect differences in the degree of cation ordering. It merely reflects differences in the signal-to-noise ratios in the experimental spectra. The better the signal-to-noise ratio, the more sensitive the mean-squared deviation of the fit will be to the assumed value of S.

An alternative interpretation of our NMR data might be that the ordered domains in the $Ga_{0.5}In_{0.5}P$ films are fully ordered, but occupy only a small fraction ($\leq 15\%$) of the sample volume. To rule out this interpretation, we obtained TEM data for sample D, using a Philips CM-30 microscope operating at 300 keV. Sample D was chosen from TEM measurements because of its comparatively small band gap and because it was grown under conditions believed to lead to a high degree of cation ordering.[14] Plan-view specimens were prepared by mechanical polishing from the substrate side and subsequent chemical thinning until perforation using 1% bromine in methanol. The specimen was tilted from the [001] zone to an orientation exhibiting superlattice reflections arising from cation ordering along both the $(\bar{1}11)$ and $(1\bar{1}1)$ planes. Figure 6(a) shows the electron-diffraction pattern. The two superlattice networks indicating cation ordering along the (111) and $(1\bar{1}1)$ planes are labeled A and B. The B variant predominates. Dark-field TEM images [Figs. 6(b) and 6(c)] were obtained using superlattice

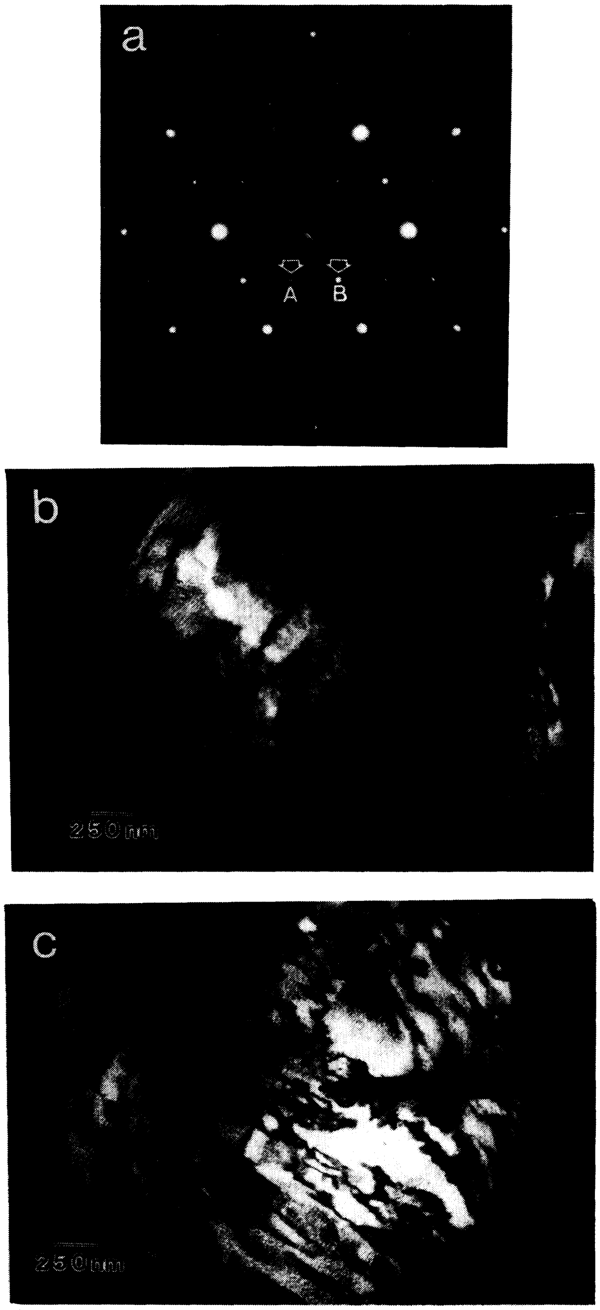

FIG. 6. (a) Electron-diffraction pattern of sample D. Superlattice reflections marked A and B arise from cation ordering along $(\bar{1}11)$ and $(1\bar{1}1)$ planes. (b) Dark-field image constructed from superlattice reflection A. (c) Dark-field image of the same area constructed from superlattice reflection B.

reflections from the two variants. The ordered domains occupy abut 75% of the total sample volume. TEM images were not obtained for samples *A*, *B*, and *C*, but earlier measurements on samples grown under similar conditions gave results similar to those in Fig. 6 for samples with low band gaps.

The analysis above assumes an assignment of the ^{31}P NMR lines in which the resonance from a $Ga_nIn_{4-n}P$ cluster shifts monotonically to higher frequencies as *n* increases. Two pieces of evidence support this assignment. First, the areas of the lines in the spectra in Figs. 2 and 3 are consistent with this assignment, i.e., good fits to the experimental spectra are obtained. Second, we find that T_2 increases monotonically with increasing frequency across the spectrum, for both $Ga_{0.5}In_{0.5}P$ and $Ga_{0.14}In_{0.86}P$. For $Ga_{0.5}In_{0.5}P$ (sample *A*), T_2 ranges from 2.7 to 5.4 ms at $\nu_{MAS}=6.0$ kHz as *n* goes from 0 to 4; for $Ga_{0.14}In_{0.86}P$, T_2 ranges from 1.2 to 1.8 ms at $\nu_{MAS}=5.0$ kHz as *n* goes from 0 to 2. We may expect T_2 in a spin-echo measurement to increase as *n* decreases because the In isotopes (spin $\frac{9}{2}$, 4.3% abundance, $\gamma=9.30$ MHz/T for ^{113}In; spin $\frac{9}{2}$, 95.7% abundance, $\gamma=9.33$ MHz/T for ^{115}In) have larger magnetic moments than the Ga isotopes (spin $\frac{3}{2}$, 60.4% abundance, $\gamma=10.22$ MHz/T for ^{69}Ga; spin $\frac{3}{2}$, 39.6% abundance, $\gamma=12.98$ MHz/T for ^{71}Ga). Spin diffusion among In nuclei should then be more rapid than spin diffusion among Ga nuclei. Rapid spin diffusion would prevent the phophorus-indium dipole-dipole couplings from being averaged out efficiently by MAS and refocused by the spin-echo sequence, leading to a shorter T_2 for ^{31}P spins that are coupled to more In spins.[24] An ^{115}In spin-lattice relaxation rate that is on the order of the sample spinning rate would also result in a shorter T_2 for ^{31}P spins with more In neighbors.

The value of the ^{31}P chemical shift for a particular $Ga_nIn_{4-n}P$ cluster apparently depends on *x*, the stoichiometry of the material. For a given *n*, the shift in $Ga_{0.5}In_{0.5}P$ is about 30 ppm less than that in $Ga_{0.14}In_{0.86}P$. On the other hand, the *relative* shifts for the various clusters appear to be largely independent of *x*, with the shift increasing by roughly 30 ppm for each unit increase of *n* in both $Ga_{0.5}In_{0.5}P$ and $Ga_{0.14}In_{0.86}P$ (see Figs. 2 and 3). We have also examined the ^{31}P NMR spectra of bulk GaP and InP. Under rapid MAS, GaP exhibits a sharp (4 ppm wide at $\nu_{MAS}=3.5$ kHz) line centered at -142 ppm, while InP exhibits a much broader (19 ppm wide at $\nu_{MAS}=4.6$ kHz) line centered at -148 ppm. These resonance positions do not agree well with the shifts of $n=4$ (for GaP) and $n=0$ (for InP) clusters in either $Ga_{0.5}In_{0.5}P$ or $Ga_{0.14}In_{0.86}P$ samples, supporting our observation that the value of the ^{31}P chemical shift for a particular cluster depends on the stoichiometry. The pronounced difference in the linewidths for GaP and InP also supports our contention that the ^{31}P lines with the smaller T_2 values in the MAS spectra of $Ga_xIn_{1-x}P$ arise from P atoms with more In neighbors.

IV. CONCLUSIONS

We have shown that it is possible to determine the relative populations of $Ga_nIn_{4-n}P$ clusters in $Ga_xIn_{1-x}P$, and hence the degree of cation ordering, from ^{31}P NMR spectra obtained with magic-angle spinning. Our spectra of $Ga_{0.5}In_{0.5}P$ thin films indicate that the order parameter that characterizes the degree of cation ordering has a value $S \leq 0.6$ in samples grown under a variety of conditions and with a range of band gaps, including samples that appear highly ordered in TEM images. This result places a constraint on any proposed mechanism for cation ordering in $Ga_{0.5}In_{0.5}P$ films. The difference between experimentally measured band-gap variations[14,18] and the band-gap depression predicted to result from complete cation ordering[17] is likely to be attributable to incomplete ordering in the real films.

The experiments described above represent an initial application of MAS NMR to the study of the structure of a semiconductor alloy thin film. The fact that we obtain resolved resonances in the ^{31}P NMR spectra that can be assigned to particular $Ga_nIn_{4-n}P$ clusters with less ambiguity than was possible in analogous earlier NMR studies of bulk II-VI semiconductor alloys[20] indicates that $Ga_xIn_{1-x}P$ is a material that is particularly well suited to NMR studies of cation ordering. ^{31}P NMR may also be a useful probe of ordering in related ternary and quaternary phosphide alloy films.

ACKNOWLEDGMENTS

We thank T. M. Duncan for useful discussions and for providing the $Ga_{0.14}In_{0.86}P$ sample, P. L. Trevor for determining its composition with x-ray fluorescence measurements, A. Kibbler for growing the $Ga_{0.5}In_{0.5}P$ films, and K. Jones for preparing TEM samples.

---

[1] T. S. Kuan, T. F. Kuech, W. I. Wang, and E. L. Wilkie, Phys. Rev. Lett. **54**, 201 (1985).

[2] O. Ueda, M. Takikawa, J. Komeno, and I. Umebu, Jpn. J. Appl. Phys. **26**, L1824 (1987).

[3] A. Gomyo, T. Suzuki, and S. Iijima, Phys. Rev. Lett. **60**, 2645 (1988).

[4] P. Bellon, J. P. Chevalier, G. P. Martin, E. Dupont-Nivet, C. Thiebaut, and J. P. Andre, Appl. Phys. Lett. **52**, 567 (1988).

[5] J. Goral, M. Al-Jassim, J. Olson, and A. Kibbler, in *Epitaxy of Semiconductor Layered Structures*, edited by R. T. Tung, L. R. Dawson, and R. L. Gunshor (Materials Research Society, Pittsburgh, 1988).

[6] C. S. Baxter, R. F. Broom, and W. M. Stobbs, Surf. Sci. **228**, 102 (1990). The uncertainties involved in quantifying TEM measurements are described in this paper.

[7] For additional references, see S. Mahajan, M. A. Shahid, and D. E. Laughlin, in *Microscopy of Semiconducting Materials, 1989*, IOP Conf. Proc. No. 100 (Institute of Physics and Physical Society, London, 1989), Sec. 3, p. 143.

[8] S. R. Kurtz, J. M. Olson, and A. Kibbler, Solar Cells **24**, 307

(1988).

[9] T. Nishino, Y. Inoue, Y. Hamakawa, M. Kondow, and S. Minagawa, Appl. Phys. Lett. **53**, 583 (1988).

[10] M. Kondow, H. Kakibayashi, S. Minagawa, Y. Inoue, T. Nishino, and Y. Hamakawa, Appl. Phys. Lett. **53**, 2053 (1988).

[11] A. Mascarenhas, S. Kurtz, A. Kibbler, and J. M. Olson, Phys. Rev. Lett. **63**, 2108 (1989).

[12] T. Suzuki, A. Gomyo, and S. Iijima, J. Cryst. Growth **93**, 396 (1988).

[13] P. Bellon, J. P. Chevalier, E. Augarde, J. P. Andre, and G. P. Martin, J. Appl. Phys. **66**, 2388 (1989).

[14] S. R. Kurtz, J. M. Olson, and A. Kibbler, Appl. Phys. Lett. **57**, 1922 (1990).

[15] S. Froyen and A. Zunger, Phys. Rev. Lett. **66**, 2132 (1991).

[16] J. E. Bernard, S.-H. Wei, D. M. Wood, and A. Zunger, Appl. Phys. Lett. **52**, 311 (1988).

[17] S.-H. Wei and A. Zunger, Appl. Phys. Lett. **56**, 662 (1990).

[18] B. T. McDermott, K. G. Reid, N. A. El-Masry, S. M. Bedair, W. M. Duncan, X. Yin, and F. H. Pollak, Appl. Phys. Lett. **56**, 1172 (1990).

[19] M. Mehring, *Principles of High Resolution NMR in Solids* (Springer-Verlag, New York, 1983).

[20] D. B. Zax, S. Vega, N. Yellin, and D. Zamir, Chem. Phys. Lett. **138**, 105 (1987); K. Beshah, D. Zamir, P. Becla, P. A. Wolff, and R. G. Griffin, Phys. Rev. B **36**, 6420 (1987). These papers describe NMR studies of bulk II-VI alloys, in which the possible mechanisms for cation ordering are, in principle, quite different from those in thin films.

[21] H. Lutgenmeier, Z. Naturforsch. **19a**, 1297 (1964).

[22] L. J. Humphries and R. E. J. Sears, J. Phys. Chem. Solids **36**, 1149 (1975).

[23] T. M. Duncan, R. F. Karlicek, W. A. Bonner, and F. A. Thiel, J. Phys. Chem. Solids **45**, 389 (1984).

[24] A. Abragam, *Principles of Nuclear Magnetism* (Oxford University, New York, 1961), Chap. XII.E(c).

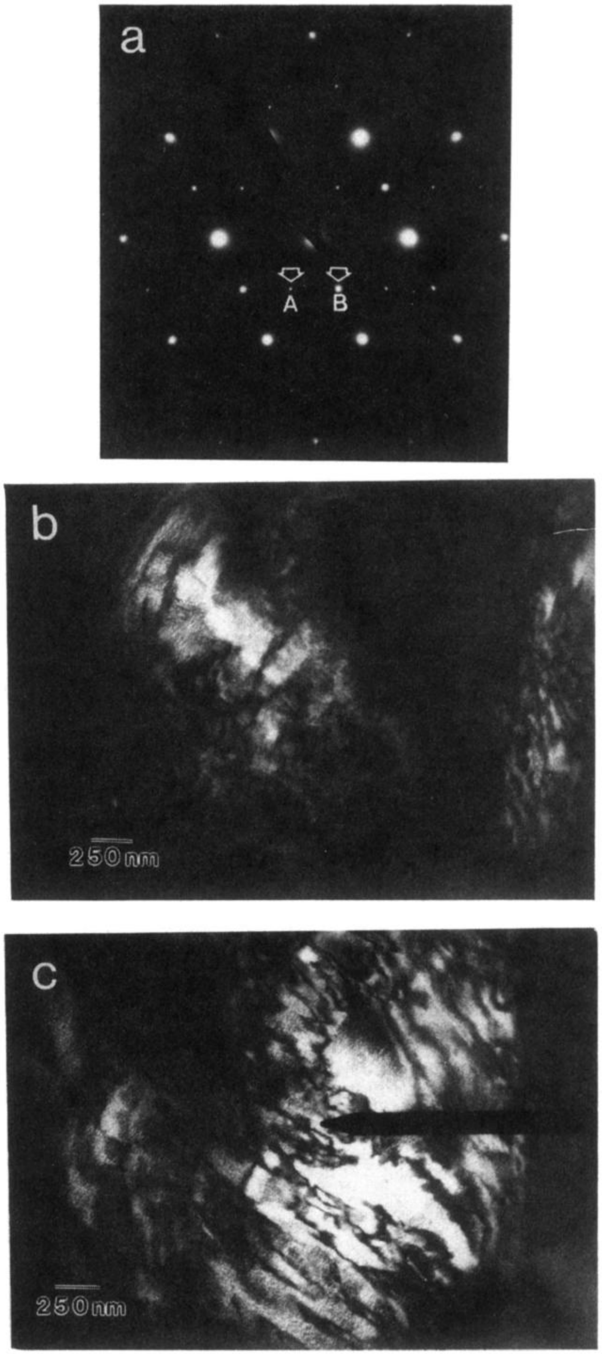

FIG. 6. (a) Electron-diffraction pattern of sample *D*. Superlattice reflections marked *A* and *B* arise from cation ordering along $(\bar{1}11)$ and $(1\bar{1}1)$ planes. (b) Dark-field image constructed from superlattice reflection *A*. (c) Dark-field image of the same area constructed from superlattice reflection *B*.